MICROSTRUCTURAL CHARACTERIZATION OF HYDROGEN-IRRADIATED 316L AUSTENITIC STAINLESS STEEL USING UNIFORM PROTON IMPLANTATION

Hlanganani Siphelele Nyembe[1)], Ezra Jacobus Olivier[1)], Alexander Sohatsky[2)], Diana Komarova[2)], Tiep Nguyen[2)], Zakhelumuzi Khumalo[3)], Christopher Mtshali[3)], Mlungisi Nkosi[3)]
[1)]*Centre for HRTEM, Nelson Mandela University, Gqeberha, South Africa, Hlanganani.Nyembe@mandela.ac.za*
[2)]*Flerov Laboratory of Nuclear Reactions, Joint Institute for Nuclear Research, Dubna, Russia, sohatsky@jinr.ru*
[3)]*Materials Research Department, NRF-iThemba LABS, Somerset West, South Africa, mlungisin@tlabs.ac.za*

This study investigates the microstructural response of 316L austenitic stainless steel (SS316L) to hydrogen loading, focusing on the role of pre-existing martensite. The use of austenitic steels in hydrogen and nuclear applications is crucial; however, their susceptibility to hydrogen embrittlement (HE), particularly in the presence of martensite, presents a significant challenge. Martensite in metastable SS316L acts as a fast diffusion pathway for hydrogen, leading to localised accumulation and increased HE susceptibility. This detrimental effect is compounded by irradiation. Samples of commercial SS316L were uniformly irradiated with 1 MeV protons at room temperature. The microstructure was characterised using SEM, EBSD, TKD and TEM techniques. Microstructural characterisation revealed an austenitic matrix with annealing twins and fine, pre-existing martensite phases in both the as-received and hydrogen-implanted conditions. The martensite is attributed to cold rolling during processing. No noticeable radiation damage was observed in the as-implanted SS316L. Post-implantation annealing and nanohardness testing will be used in future work to further investigate how the irradiation and hydrogen affects the microstructure and HE.

Keywords: austenitic stainless steel; martensite; hydrogen embrittlement; proton irradiation; radiation damage.

Introduction

Austenitic stainless steels are vital for hydrogen and nuclear applications, yet hydrogen embrittlement (HE) poses a critical challenge by degrading mechanical properties through atomic hydrogen accumulation at microstructural trap sites. A key issue is the susceptibility of metastable austenitic stainless steels to strain-induced martensitic transformation during processing. Pre-existing martensite forms fast hydrogen diffusion pathways, increasing HE and crack initiation, and reducing mechanical strength. Irradiation further exacerbates these localised deformation processes [1,2].

The current study employs uniform bulk ion-implantation to introduce hydrogen into SS316L. This approach allows for homogeneous hydrogen distribution and the critical simultaneous investigation of irradiation damage and HE [3].

This paper examines hydrogen-irradiated SS316L, focusing on pre-existing martensite. SEM-BSE, EBSD, TKD, and TEM were used for microstructural analysis [4]. EBSD mapped phases. TKD provided higher resolution phase and orientation mapping. TEM enabled detailed analysis and defect observation.

Future research will investigate the combined effects of hydrogen and irradiation on the microstructure through post-implantation annealing and nanohardness testing to understand localised mechanical property changes in both austenite and martensite phases.

Experimental

Commercial SS316L was used for this work. The typical chemical composition (in wt%) of SS316L is: 16-18 Cr, 10-14 Ni, 2-3 Mo, 2 Mn, 1 Si, 0.03 C, 0.045 P, 0.03 S, 0.1 N, and (balance) Fe. The surface of SS316L samples in the form of 5×5 mm^2 plates was polished to a colloidal silica finish (50 nm).

Samples were irradiated with a 1 MeV

proton beam at room temperature using a uniform bulk ion-irradiation methodology [1] at NRF iThemba LABS. The SRIM program [2] calculated a proton range of ~5 μm, with an expected implanted hydrogen concentration of ~0.09 at%. As-received SS316L served as the reference.

Microstructural characterization was performed using Scanning Electron Microscopy (SEM) based techniques. SEM-BSE imaging was performed at 15 kV. Electron Backscatter Diffraction (EBSD) mapping (20 kV, 70° tilt, 200 nm step size) was used to identify austenite and martensite phases. Focused Ion Beam (FIB-SEM) was used to prepare lamella samples from both phases for Transmission Kikuchi Diffraction (TKD) and Transmission Electron Microscopy (TEM). TEM analysis lamellas were performed using a JEOL JEM 2100 microscope with a LaB_6 electron gun operated at 200 kV. TKD characterisation was performed using the 30 kV accelerating voltage and 20 nm step size. TKD and EBSD data were processed using the MTEX toolbox [6].

Results

Figure 1 displays the SEM-BSE image of the as-received SS316L, revealing a typical austenitic steel microstructure with characteristic annealing twins. Both as-received and as-implanted SS316L showed similar microstructures in SEM-BSE.

Figure 2 presents an EBSD phase map of the implanted SS316L, showing a predominantly austenitic (Iron fcc) microstructure with fine martensite (Iron bcc) phases present within austenite grains. No observable differences were noted between as-received and implanted SS316L.

Low magnification BF-TEM image of the irradiated 316L steel is shown in Fig. 3. The irradiation damage was not observed on the microstructure. Both, as-received and implanted SS316L exhibited similar microstructures under TEM.

Figure 4 displays TKD phase (a) and orientation (b) maps. Similar to EBSD, TKD

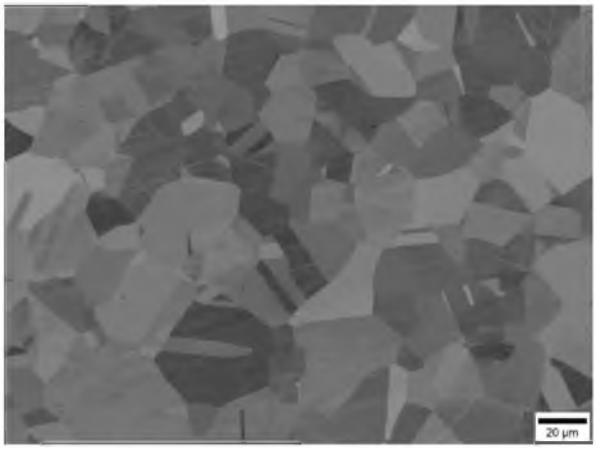

Fig. 1. SEM-BSE image of the as-received SS316L

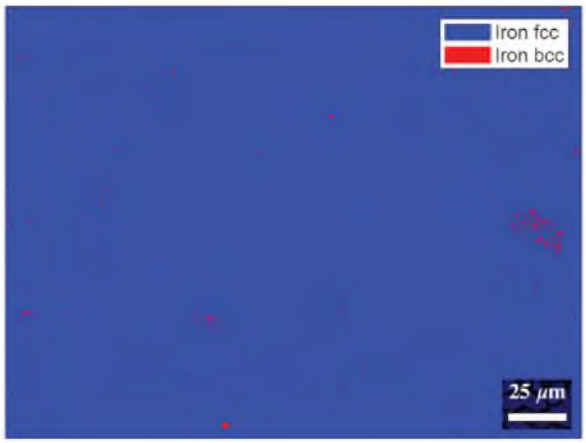

Fig. 2. EBSD phase map (austenite – Iron fcc and martensite – Iron bcc) of the implanted SS316L

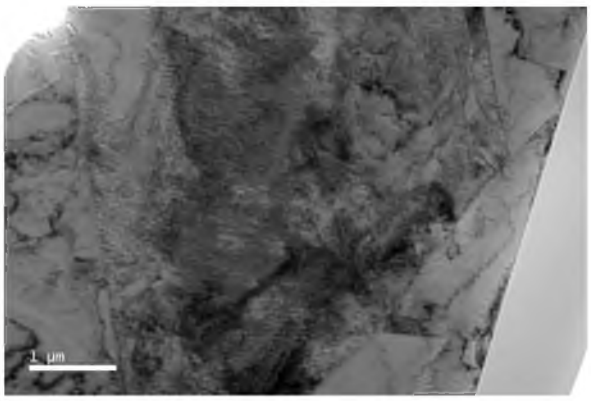

Fig. 3. BF-TEM image of the implanted SS316L

confirmed the presence of martensite (Iron fcc) within austenite grains. Orientation maps revealed slight variations within martensite grains, while austenite grains maintained uniform orientation. Microstructures of as-received and implanted SS316L were consistent.

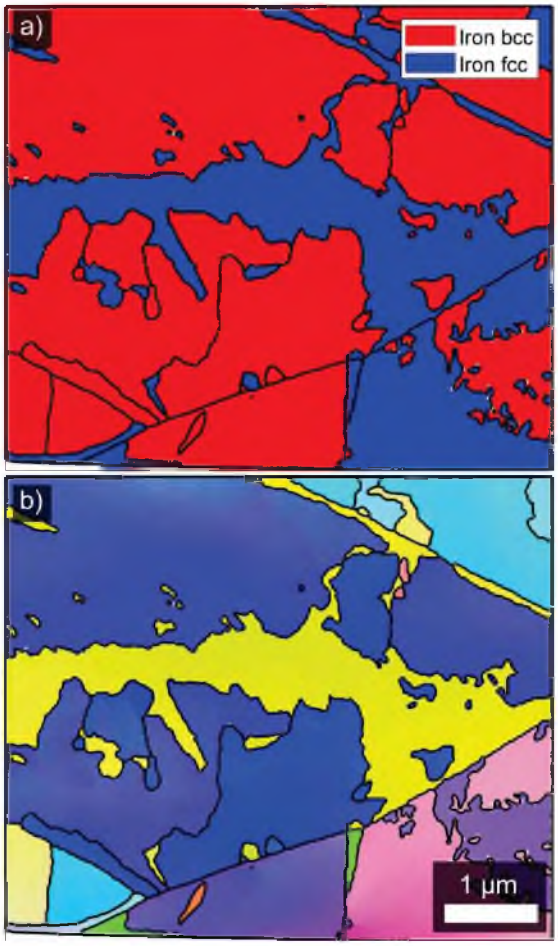

Fig. 4. TKD phase (a) and orientation (b) maps of the implanted SS316L

Discussion

The SEM-BSE analyses consistently revealed a dominant austenitic microstructure with characteristic annealing twins, typical for SS316L steel. EBSD confirmed the presence of fine martensite phases within the austenite grains, observed in both the as-received and implanted SS316L. This indicates that the martensite was pre-existing, likely formed during the cold rolling process of the SS316L steel plates. The observed slight variation in orientation within the martensite grains, as detected by TKD, further supports its formation via deformation-induced mechanisms. Despite the hydrogen implantation, TEM evaluations of the SS316L did not reveal noticeable radiation damage to the microstructure in the as-implanted state. The lack of post-implantation annealing in this study explains the absence of visible radiation damage.

Conclusion

This study confirmed the presence of a pre-existing martensite phase in both as-received and hydrogen-implanted SS316L. While the hydrogen implantation did not result in readily observable radiation-induced microstructural damage in the as-implanted state, further studies including post-implantation annealing and nanohardness testing of the SS316L are planned to investigate the combined effects of hydrogen and irradiation on the microstructure of SS316L, particularly focusing on the behavior of the pre-existing martensitic phase.

Acknowledgments

The National Research Foundation of South Africa is acknowledged for financial support (Grant Number TTK240316209461). The NRF-iThemba LABS is acknowledged for performing proton irradiation experiments.

References

1. Fan Z., Gong X., Li B., Yu P., Liu X., Zhou H., He Y., et al. The formation of strain-induced martensite and its influence on hydrogen compatibility of metastable austenitic stainless steels: A state-of-knowledge review. *Journal of Science: Advanced Materials and Devices* 2025; 10: 100842.
2. Wharry J.P., Mao K.S. The role of irradiation on deformation-induced martensitic phase transformations in face-centered cubic alloys. *Journal of Materials Research* 2020. DOI: 10.1557/jmr.2020.80.
3. Sohatsky A.S., Komarova D.A., Nguyen T.V., Skuratov V.A., Mitrofanov S.V., Khumalo Z.M., et al. Novel methodology of homogeneous ion doping/damage of nuclear materials for structural characterization. *Journal of Nuclear Materials* 2025; 606: 155601. https://doi.org/10.1016/j.jnucmat. 2025.155601.
4. Nyembe H.S., van der Meer P., Knutsen R., et al. Microstructure-Based Creep Life Assessment of 1CrMoV Turbine Rotor Steels After Long-Term Service. *J Fail. Anal. and Preven.* 2024; 24, 559-574.
5. Zeigler, J.F., Biersack, J.P. The stopping and range of ions in matter. In: Bromley, D.A. (Ed.), Treatise heavy-ion Sci. Boston: Springer; 1985.
6. Bachmann F., Hielscher R., Schaeben, H. Texture analysis with MTEX–free and open source software toolbox. *Solid State Phenomena* 2010; 63-68.